



Breaking barriers: The novel *in vitro* microdialysis system enables reproducing *in vivo* extraction efficiencies of linezolid

Felix Leon Müller^{a,b} , Davide Bindellini^a, Gerd Mikus^{a,c}, Robin Michelet^{a,*}, Charlotte Kloft^{a,b,*}

^a Department of Clinical Pharmacy and Biochemistry, Institute of Pharmacy, Freie Universitaet Berlin, Kelchstrasse 31 12169 Berlin, Germany

^b Graduate Research Training Program PharMetX, Berlin Potsdam, Germany

^c Department of Clinical Pharmacology and Pharmacoepidemiology, University Hospital Heidelberg, Im Neuenheimer Feld 419 69120 Heidelberg, Germany

ARTICLE INFO

Keywords:

Microdialysis calibration
Relative recovery
Diffusion
Permeability
Extraction efficiency
In vitro systems
Linezolid

ABSTRACT

Reported extraction efficiencies (EE) of the minimally invasive microdialysis (μ D) technique for linezolid (LIN) varied in subcutaneous adipose tissue of obese 42.8 % (95 %CI:35.9 %-50.2 %) and non-obese patients 61.0 % (95 %CI:54.4 %-67.1 %). EE must be determined *in vivo*, as *in vitro* μ D systems (EE=94.1 % for LIN) so far fail to reflect *in vivo* processes and conditions. This study aimed to develop an *in vitro* μ D system capable of reproducing *in vivo* EE of LIN for different populations by mimicking tissue characteristics and processes limiting EE. Based on the static *in vitro* μ D system two novel systems were developed: (i) mimicking catheter surrounding as artificially tissue structure (aTS) by creating a porous matrix using milling beads, and (ii) adding a surrounding flow as artificial tissue perfusion (aTP) through the aTS. While experiments using the aTS μ D system resulted in a low EE of 33.2 % (95 %CI=31.8 %-34.7 %), adding aTP increased EE in a function of aTP, to a maximum of 97.2 % (95 %CI=91.1 %-104 %). The aTP μ D system successfully reproduced the median reported *in vivo* EE range for LIN, matching EE for obese and non-obese at an aTP of 0.013 and 0.061 mL/min, respectively. By reproducing *in vivo* EEs for LIN, the novel aTP μ D system (aTPMS) provides a platform for optimising μ D settings in clinical trials, with future studies needed to explore its application to other substances.

1. Introduction

The *in vivo* microdialysis (μ D) technique is the gold standard (De La Pena et al., 2000; Plock and Kloft, 2005) to determine the pharmacokinetics (PK) directly at the site of action for antibiotics, which is for most bacteria-antibiotic interaction the interstitial space fluid (ISF) of e. g., lung, liver, bone, subcutaneous (sc.) adipose tissue and brain. The diffusion driven μ D technique is recommended for drugs, when a direct translation from plasma PK to the target-site PK is not possible due to differences between the unbound plasma concentration-time profiles and the observed concentrations in ISF (C_{ISF}), e. g., for linezolid (LIN) and meropenem (Busse et al. 2021; Busse et al., 2021b; Ehmann et al., 2020). Thus, the target-site related PK should be used as surrogate to predict the antibiotic effect (Craig and Middleton, 1998; Marchand et al., 2016; Ryan, 1993; van Os et al., 2024; van Os and Zeitlinger, 2021). Microdialysis catheters consist of a semipermeable membrane connected to an inflow and outflow for the perfusate, which is pumped through the catheter at rates between 0.5 to 5 μ L/min (Plock and Kloft, 2005). In

clinical studies, drug molecules in the ISF diffuse across the membrane into the perfusate and samples, so-called dialysates, are collected at the outlet over certain time intervals. Due to the constant perfusate flow through the catheter an equilibrium between drug concentration in the perfusate and catheter sampling site in the ISF is not achieved and only a fraction from C_{ISF} is extracted and quantified as μ D concentration (C_{Dial}), characterising the extraction efficiency (EE) of the catheter. EE from the tissue ISF into the catheter, commonly described as relative recovery (RR), cannot be determined directly. Protein binding and unspecific binding of the drug of interest in the ISF, as well as difficulties to extract ISF without damaging cells technically preclude the determination of the true, unbound C_{ISF} , thus EE (Deitchman et al., 2018; Nation et al., 2018; Nilsson, 2013). Consequently, for each catheter the EE needs to be determined via catheter calibration to enable the calculation of C_{ISF} from C_{Dial} . Of the existing calibration methods (Bungay et al., 2006; Kho et al., 2017; Stenken, 1999) the most common one in clinical trials is the retrodialysis technique, in which the perfusate is replaced by the retro-perfusate containing a high concentration of the drug of interest. By conducting retrodialysis calibration the EE is determined, termed

* Corresponding author: Freie Universitaet Berlin, Institute of Pharmacy, Department of Clinical Pharmacy and Biochemistry, Kelchstr. 31 12169 Berlin, Germany.
E-mail addresses: robin.michelet@fu-berlin.de (R. Michelet), charlotte.kloft@fu-berlin.de (C. Kloft).

<https://doi.org/10.1016/j.ejps.2025.107085>

Received 19 September 2024; Received in revised form 19 February 2025; Accepted 29 March 2025

Available online 29 March 2025

0928-0987/© 2025 Published by Elsevier B.V. This is an open access article under the CC BY-NC-ND license (<http://creativecommons.org/licenses/by-nc-nd/4.0/>).

Abbreviations			
aTP	Artificial tissue perfusion	ISF	Interstitial space fluid
aTP _{EE50}	Artificial tissue perfusion at half maximal extraction efficiency	LIN	Linezolid
aTPMS	Artificial tissue perfusion microdialysis system	MB	Milling beads
aTSMS	Artificial tissue structure microdialysis system	μ D	Microdialysis
C _{Dial}	Microdialysis concentration	PK	Pharmacokinetic
C _{ISF}	Interstitial space fluid concentration	RR	Relative recovery
C _{Per}	Retroperfusate concentration	rD	Relative delivery
D _t	Diffusion coefficient in tissue	rD _{aTP}	Relative delivery from the aTPMS
EE	Extraction efficiency	rD _{aTS}	Relative delivery from the aTSMS
EE _{Base}	Baseline extraction efficiency	rD _{REF}	Reference relative delivery
EE _{Max}	Maximal extraction efficiency	RR _{aTP}	Relative recovery from the aTPMS
HPLC-UV/VIS	High-performance liquid chromatography ultraviolet/visible	RR _{aTS}	Relative recovery from the aTSMS
		RR _{REF}	Reference relative recovery
		RS	Ringer's solution
		s.c.	Subcutaneous
		sIVMS	Static <i>in vitro</i> microdialysis system

relative delivery (rD), *i.e.* extraction of molecules from the retroperfusate into the tissue ISF. Indeed, as diffusion kinetics across the membrane are assumed to be independent from the direction of diffusion, RR is assumed to equal rD (Zhao et al., 1995) and C_{Dial} are converted to C_{ISF} by dividing by rD when the system is in steady-state (Bungay et al., 2001).

The oxazolidinone antibiotic linezolid (LIN) has been well studied in the ISF of different tissues using μ D (Andreas et al., 2015; Dehghanyar et al., 2005; Eslam et al., 2014; Gee et al., 2001; Schwameis et al., 2017; Stolle et al., 2008; Thallinger et al., 2008; Wiskirchen et al., 2011). Its EE depends on perfusate flow, membrane (type), length of the catheter, and the permeability of the drug in the catheter-surrounding matrix. Tissue ISF permeability, *i.e.* movement of molecules in the ISF, can exhibit patient-specific variability, which can lead to lower EE in specific sub-populations: For LIN, *in vivo* EE in subcutaneous adipose ISF of 42.8 % (95 %CI:35.9 %–50.2 %) for obese patients and 61.0 % (95 %CI:54.4 %–67.1 %) for non-obese were determined (Busse et al., 2021a), compared to observed *in vitro* EE between 90.2–97.9 % (Burau et al., 2019). *In vivo*, tissue characteristics and structure have been shown to restrict the permeability of substances, depending on the substance diffusion coefficient in the tissue (D_t), tissue perfusion and drug elimination from the tissue. Typically, when tissue permeability is lower than that of the μ D catheter, it becomes the limiting factor for EE (Bungay et al., 2006; Chen et al., 2002). *In vitro*, however, the catheter-surrounding matrix, typically a well-stirred ISF-like solution, is considered to not restrict permeability, and only catheter membrane permeability limits EE. These differences imply that *in vitro* systems in their current state are not capable of reproducing median reported *in vivo* EE. Yet, the use of *in vitro* systems is highly recommendable to perform feasibility studies prior clinical μ D studies. Currently, an evidence-based optimisation of μ D settings to ensure sufficient EE *in vivo* is not possible and relies on the expertise of clinical personnel. An *in vitro* μ D system predicting *in vivo* EE is currently not available and would help support evidence-based recommendations for clinical μ D settings, thereby fostering the usage of μ D in clinical studies. The aim of this study was thus to (i) develop an *in vitro* μ D system that reproduces *in vivo* EE for different populations by mimicking D_t and tissue perfusion using LIN as a model substance, and (ii) compare the resulting EE to published *in vivo* data of LIN in different study populations.

2. Materials and methods

2.1. Materials

Linezolid was obtained from Pfizer (Peapack, New Jersey, USA). Acetonitrile of analytical grade was obtained from VWR Chemicals

(Fontenay-sous-Bois, France) and ultra-pure water was generated using a Millipak® system (Merck Millipore, Darmstadt, Germany). Sterile Ringer's solution (RS) was obtained from B. Braun Melsungen AG (Melsungen, Germany). CMA 63 catheters and CMA/102 pumps were purchased from mDialysis and CMA/Microdialysis AB, respectively (both in Stockholm, Sweden). 1 mL Omnix syringes fitting the μ D pumps were purchased from B. Braun SE (Melsungen, Germany). Safe-lock vials (0.5–1.5 mL), as well as adjustable pipettes and tips (20–1000 μ L), were sourced from Eppendorf (Hamburg, Germany). Milling beads (MB) with diameters of 200–300 μ m (SiLibeads, Sigmund Lindner, Warmensteinach, Germany), 100 μ m and 200 μ m (Power Beads, Hosokawa Alpine, Japan), and 50 μ m diameter (Bühler, Uzwil, Switzerland) were used. A magnetic stirrer (RCT basic) from IKA Labortechnik GmbH (Staufen, Germany), and a Sonorex Digitec ultrasonic bath (Typ DT 106) from Bandelin Electronic (Berlin, Germany) were used. The ISMATEC MV-CA 4 pump from Cole-Parmer GmbH (Wertheim, Germany) was used in combination with Tygon LMT-55 stopper tubing (IDEX Health & Science GmbH, Wertheim, Germany) and Tygon LMT extension tubing (Carl Roth, Karlsruhe, Germany) (further specification see supplements 7.1).

2.2. General *in vitro* μ D set up

The static *in vitro* μ D system (sIVMS) (Simmel et al., 2013) was used as the basis to develop *in vitro* artificial tissue μ D systems and to determine reference EE (Section 2.3). The sIVMS consisted of a test tube (volume of 15 mL) holder with a heating block to maintain the temperature at 37 °C. In each experiment, μ D catheters were connected to 1 mL Omnix syringes. CMA/102 pumps were used throughout all experimental settings to apply the perfusate flow through the catheter. CMA 63 catheters with a molecular mass cut-off of 20 kDa and a membrane length of 30 mm were used, corresponding to catheters used *in vivo* for LIN (Dehghanyar et al., 2005; Eslam et al., 2014; Gee et al., 2001; Stolle et al., 2008; Thallinger et al., 2008).

2.3. Reference extraction efficiencies in the sIVMS

EE reference values (RR_{REF} and rD_{REF} for microdialysis and retrodialysis, respectively) were determined at optimal (well-stirred) conditions of the catheter surrounding matrix. The catheters were inserted into a test tube containing 14 mL of a well-stirred C_{ISF}=6 μ g/mL LIN in RS corresponding to clinically relevant maximal LIN concentration (Ehmann et al., 2020) (Fig. 1A). As retroperfusate (C_{Per}), RS with C_{Per}=60 μ g/mL or C_{Per}=80 μ g/mL LIN was used. To determine RR_{REF} and rD_{REF}, 23 experiments were performed according to the schedule in Fig. 2.

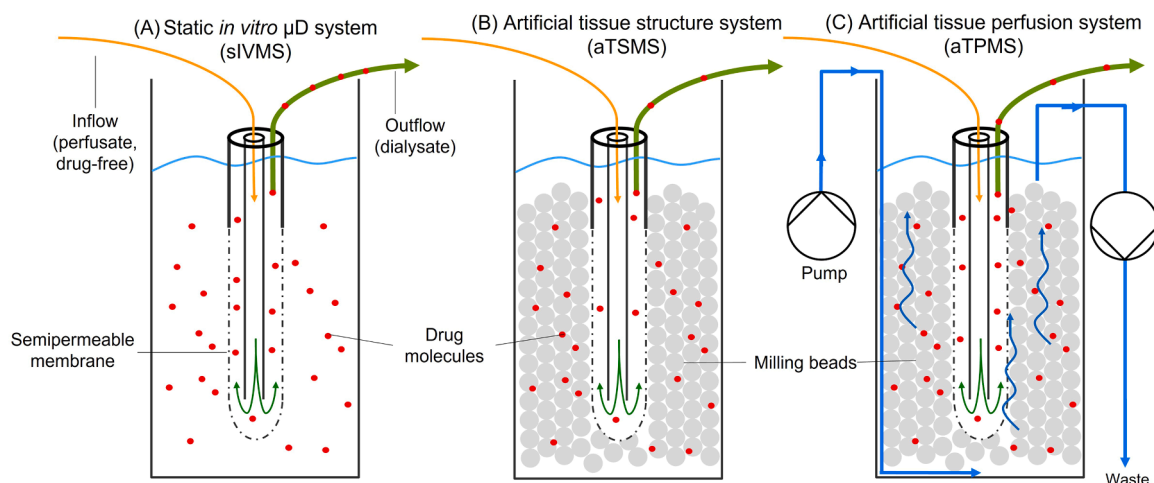


Fig. 1. Schematic of three experimental microdialysis systems; (A) reference experiment in the static *in vitro* μD system (sIVMS), (B) artificial tissue structure μD system (aTSMS) with milling beads, and (C) artificial tissue perfusion μD system (aTPMS) with surrounding milling beads; red circles: drug molecules, grey circles; milling beads.

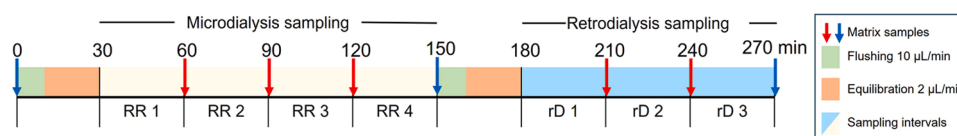


Fig. 2. Sampling schedule for all experiments: from 30 to 150 min: microdialysis setting; from 180 to 270 min: retrodialysis setting blue arrows: catheter-surrounding matrix samples taken in all systems (sIVMS, aTSMS, aTPMS); red arrows: catheter-surrounding matrix samples taken from the artificial tissue perfusion microdialysis system (aTPMS). Abbreviations: aTSMS: artificial tissue structure microdialysis system; sIVMS: static *in vitro* microdialysis system; rD: relative delivery; RR: relative recovery.

2.4. Artificial tissue structure system (aTSMS)

To mimic the tissue structure of the *in vivo* ISF of the target site around the catheter, inert milling beads (MB) made from yttrium-stabilized zirconium with diameters of 200–300 μm SiLibaed (referred to as 250 μm), 100 μm and 200 μm Power Beads, and 50 μm MB were used (Fig. 1B). A $C_{ISF}=6 \mu\text{g/mL}$ LIN in RS was mixed with 100 g of MB. To remove remaining air from the submerged MB, the solution was stirred and degassed using an ultrasonic bath until no more air bubbles emerged from the MB. The filling procedure started by placing a 10 cm long straw in the test tube from the sIVMS as placeholder for the catheter and 3 mL of C_{ISF} solution of 6 μg/mL LIN in RS was added. With a spatula, the degassed MB were added around the straw until ¾ of the test tube was filled. The catheter was inserted into the straw which was carefully removed from the MB without pulling the catheter. If the membrane was not completely submerged in the MB, the procedure was repeated starting from the filling of the test tube. The samples of the C_{ISF} solution were taken from liquid above the MB to not alter processes within the MB matrix and to prevent damaging catheters. As retroperfusate $C_{Per}=60 \mu\text{g/mL}$ LIN in RS was used. A total of 60 experiments were conducted, with 15 experiments for each MB diameter to determine RR_{aTS} and rD_{aTS} , following the sampling schedule in Fig. 2.

2.5. Artificial tissue perfusion system (aTPMS)

To mimic the tissue perfusion, a flow through aTSMS was added (Fig. 1C), referred to as artificial tissue perfusion (aTP). In the aTPMS, 50, 100, and 250 μm MB diameters were used and aTP was controlled using a peristaltic pump and Ismatec Tygon tubes with an inner diameter of 0.51 mm. Compared to the aTSMS, an adapted filling procedure of the test tubes was applied utilising the peristaltic pump: First, the inflow spiral-tube was placed at the bottom of the test tube and the straw was

inserted. Second, dry MB were added, and the inflow was connected to the peristaltic pump set to a high flow rate of ~1 mL/min of catheter surrounding solution. During the filling the placeholder straw and spatula were used to stir the MB ensuring constant filling without air stuck in the MB matrix. Third, the catheter was then inserted into the straw the same way as described above for the aTSMS (Section 2.4). To keep the volume of the catheter surrounding solution within the system constant, excess solution above the MB was withdrawn at the same pump rate as the inflow (Fig. 1C).

Before each experiment, the flow rate of the peristaltic pump was determined ($n = 2$). Flow rates from 0.05 to 0.5 mL/min were set, as well as $C_{ISF}=6 \mu\text{g/mL}$ and retroperfusate of $C_{Per}=80 \mu\text{g/mL}$ LIN in RS were used. Retrodialysis, μD and matrix samples (LIN in RS) were taken according to the schedule in Fig. 2.

2.6. General experimental settings of μD and retrodialysis investigations

Before each experiment and when switching from μD to retrodialysis, flushing with an initial perfusate flow of 10 μL/min for 10 min followed by an equilibration phase with perfusate flow of 2 μL/min for 20 min was applied. Perfusate flow throughout sampling phase was 2 μL/min. In total, per experiment 4 μD samples and 3 retrodialysis samples of 30 min intervals over 2 and 1.5 h, respectively, were collected (Fig. 2). To prevent evaporation the samples were collected in 0.5 mL safe lock vials on ice. After every experiment, the catheters were carefully removed from the matrix, inserted into ultra-pure water, and flushed with ultra-pure water at 10 μL/min for at least 30 min. All μD, retrodialysis and matrix LIN samples were stored at 8 °C and analysed directly after the experiment using a validated HPLC-UV/VIS assay (Buerger et al., 2003) and EE (*i.e.* RR and rD) was calculated according to Eq. (1):

$$EE = \frac{(C_{Per} - C_{Dial})}{(C_{Per} - C_{ISF})} \quad (1)$$

with C_{Per} being the perfusate, C_{Dial} the dialysate and retrodialysate, and C_{ISF} the unbound LIN concentration in the *in vivo* ISF or *in vitro* catheter surrounding matrix. In case of microdialysis setting, C_{Per} was equal to 0 and the equation for EE, corresponding to RR, simplified to

$$RR = \frac{C_{Dial}}{C_{ISF}} \quad (2)$$

For rD, when C_{ISF} is 0, i.e. at the start of the experiment, the equation for EE simplified to

$$rD = 1 - \frac{C_{Dial}}{C_{Per}} \quad (3)$$

otherwise, Eq. (1) needs to be used.

2.7. Statistical analysis

All resulting EE and C_{ISF} were analysed using R v. 4.3.1 (R Foundation for Statistical Computing, Vienna, Austria). Relationship between aTP and EE was investigated using nonlinear regression utilising the nlme package. The corresponding RR and rD values were compared using paired *t*-tests, while comparisons of EE between reference values and aTSMs were performed using unpaired *t*-tests. A significance level of $\alpha=0.05$ was applied for all statistical tests.

3. Results

3.1. Reference experiments using sIVMS

RR_{REF} and rD_{REF} were determined in 23 experiments yielding 92 microdialysis and 69 retrodialysis samples using 7 catheters. The mean value derived from each experiment (per day and catheter) were $89.9 \pm 6.4\%$ for RR_{REF} and $91.5 \pm 4.5\%$ for rD_{REF} . No significant difference was found between RR_{REF} and rD_{REF} (mean difference: -2.1% , 95% CI = $-5.5\% - 1.2\%$, *p*-value = 0.16) (Fig. 3, green crosses). The EE remained constant over time (Fig. 4, top left panel, green circles).

3.2. Artificial tissue structure system (aTSMs)

In total, EE from 60 experiments were collected (240 microdialysates and 180 retrodialysates), and data from three experiments were discarded due to membrane leakage; these broken catheters were replaced in the subsequent experiment. Furthermore, seven experiments were excluded when the difference between RR and rD was larger than $\pm 10\%$ points, i.e., data analysis comprised 50 experiments.

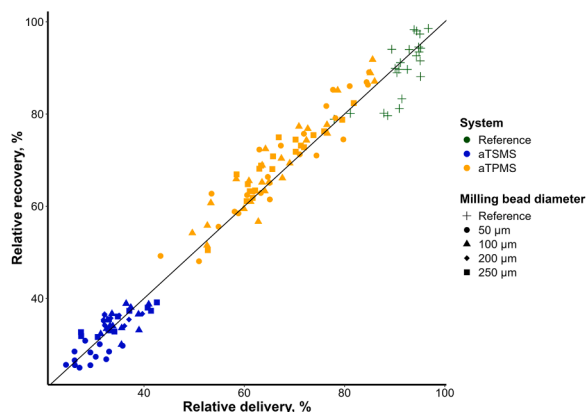


Fig. 3. Relative delivery versus relative recovery determined in the (i) reference system (green, $n = 23$ experiments), (ii) artificial tissue structure microdialysis system (aTSMs, blue, $n = 50$ experiments) and (iii) artificial tissue perfusion microdialysis system (aTPMS, yellow, $n = 73$ experiments) with the line of identity; symbols: diameter size of milling beads.

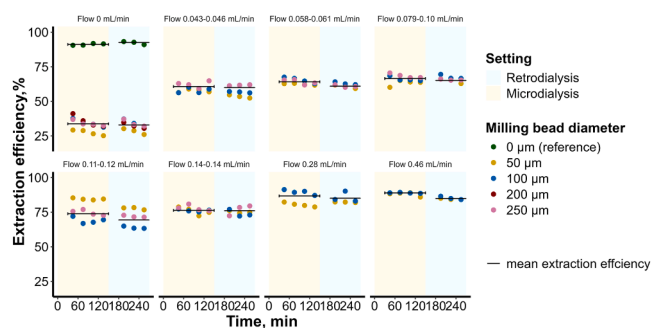


Fig. 4. Extraction efficiency over time in all *in vitro* systems, representing relative recovery (yellow area) and relative delivery (blue area), experiments grouped by the applied artificial tissue perfusion; top left panel: extraction efficiencies from reference system (green circles) and artificial tissue structure system, lines: mean extraction efficiency.

The LIN nominal C_{ISF} of $6 \mu\text{g/mL}$ remained constant during the experiment's duration of 270 min ($n = 52$, start = $6.5 \pm 0.48 \mu\text{g/mL}$, end = $6.6 \pm 0.62 \mu\text{g/mL}$, Figure S1) and RR_{aTS} and rD_{aTS} matched well (Fig. 3, blue symbols). The mean RR_{aTS} and rD_{aTS} per catheter and MB diameter (Fig. 5) were compared using a paired *t*-test and no significant differences were found: For $50 \mu\text{m}$, RR_{aTS} and rD_{aTS} were 30.8% and 29.9% (*p*-value = 0.058), for $100 \mu\text{m}$ 34.8% and 35.3% (*p*-value = 0.53), for $200 \mu\text{m}$ 35.4% and 34.0% (*p*-value = 0.088), and for $250 \mu\text{m}$ 34.9% and 34.6% (*p*-value = 0.72), respectively. Compared to the reference experiments a significant decrease of total 56.8% points for RR_{aTS} and 58.2% points for rD_{aTS} (*t*-tests, *p*-values < 0.001) was observed. Between the MB, a significant difference was found between EE of $50 \mu\text{m}$ and all other MB diameters (unpaired *t*-tests; *p*-value < 0.021). In contrast, there were no significant differences between EE of 100, 200, and 250 μm MB.

Furthermore, in microdialysates a decreasing and in retrodialysates an increasing LIN concentration over time was notable across all MB diameters, thus, overall mean RR_{aTS} and rD_{aTS} decreased over time from $36.4 \pm 4.6\%$ to $30.3 \pm 3.8\%$ and $36.0 \pm 5.3\%$ to $30.9\% \pm 4.5\%$, respectively (Fig. 4, top left panel and Figure S2).

3.3. Artificial tissue perfusion system

In 82 experiments, RR_{aTP} (from 328 microdialysates) and rD_{aTP} (from 246 retrodialysates) from 6 catheters were determined. 9 experiments were excluded due to difference $> \pm 10\%$ points between RR_{aTP} and rD_{aTP} ($n = 5$) or catheter malfunction ($n = 4$) resulting in 73 experiments for data analysis. In general, both EE values agreed well as shown in

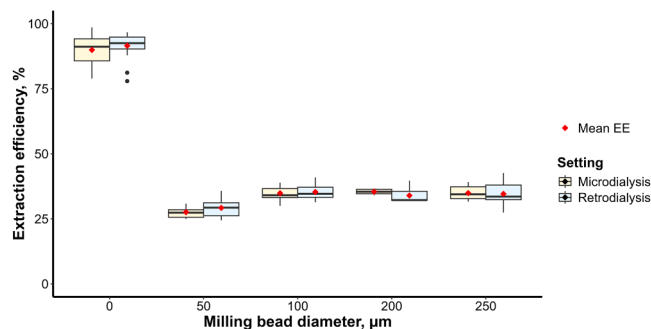


Fig. 5. Extraction efficiency (EE) representing relative recovery in a microdialysis setting (blue) and relative delivery in a retrodialysis setting (yellow) for reference experiments (" $0 \mu\text{m}$ ") and different milling bead diameters; box: interquartile range (IQR), 25th and 75th percentile with the median shown as horizontal line and mean as red diamond; whiskers: 1.5-times the IQR below the 25th percentile and above the 75th percentile, respectively; full circles: indicate extraction efficiencies values outside the IQR.

Fig. 3 (yellow symbols).

The applied aTP kept LIN C_{ISF} solution nominal concentrations of 6 µg/mL constant during microdialysis with an overall mean of 6.1 ± 0.43 µg/mL (Figure S3). During the retrodialysis setting, the LIN C_{ISF} solution of 6.1 ± 0.43 µg/mL initially increased over the sampling period before reaching a plateau at 7.0 ± 0.85 µg/mL at 240 min, for all but the two highest aTP which remained constant at 5.4 ± 0.35 µg/mL (Figure S3). The EE values were constant over time (Fig. 4). The lowest EE values in the aTPMS was 57.0 ± 6.3 % (rD) at the lowest aTP of 0.043–0.046 mL/min and highest EE was 87.9 ± 1.4 % (RR) at aTP of 0.463 mL/min. Furthermore, standard deviation was similar throughout reference setting, aTSMS, and aTPMS with a maximum of 6.6 %, 4.2 % and 7.4 %, respectively (Table 1). The trend that the 50 µm diameter MB showed a lower EE as in the aTSMS was not observed and between the 50, 100, and 250 µm MB no significant difference was observed at similar aTP below 0.14 mL/min (pairwise *t*-test, *p*-value > 0.092). At aTP ≥ 0.28 mL/min, pairwise *t*-tests were not conducted considering the small number of data points of *n* = 2–4 (Table 1).

3.4. Relationship between EE and aTP

The EE in the aTPMS increased with increasing aTP, and remained within the range of determined EE from the reference system and the aTSMS (Fig. 6). Using nonlinear regression, the increase of EE was best described by a saturable relationship represented in a sigmoidal model, according to Eq. (4):

$$EE(aTP) = EE_{Base} + \left(\frac{(EE_{Max} - EE_{Base}) \cdot aTP}{aTP_{EE50} + aTP} \right) \quad (4)$$

where EE represented either RR or rD, the subscript Base and Max denotes the baseline and maximum EE, respectively, and aTP_{EE50} the aTP when the half-maximal EE was reached. Nonlinear regression for EE vs. aTP for each MB diameter revealed negligible differences (Figure S4), thus the EE from all experiments conducted in the aTSMS and aTPMS was used without stratification for MB diameters.

Estimated EE_{MAX} was 97.2 % (95 %CI=91.1 %–104 %) and 93.4 % (95 %CI=87.4 %–101 %), for RR_{aTP} and rD_{aTP}, respectively. EE_{Base} for RR_{Base} was 33.2 % (95 %CI=31.8 %–34.7 %) and for rD_{Base} 33.3 % (95 %CI=31.9 %–34.7 %). The aTP needed to reach the half-maximal RR₅₀ of 65.3 % (95 %CI=60.6 %–69.4 %) was 0.070 mL/min (95 %CI=0.052–0.091 mL/min) compared to the half-maximal rD₅₀ of 63.4 % (95 %CI=58.7 %–66.6 %) with a similar flow of 0.071 mL/min (95 %CI=0.052–0.088 mL/min). At flow rates > 0.39 mL/min 90 % of the RR_{MAX} and rD_{MAX} was reached (87.6 % RR_{MAX}; 84.1 % rD_{MAX}).

Table 1

Extraction efficiencies, *i.e.*, relative recovery and relative delivery for experiments in the reference, artificial tissue structure and artificial tissue perfusion (by pump rate) systems with the respective standard deviation.

aTP [mL/min]	System	n*	Relative delivery		Relative recovery	
			Mean, %	SD, %	Mean, %	SD, %
0	Reference	23	91.5	4.5	89.9	6.6
0	aTSMS	50	33.3	4.2	33.1	3.9
0.043-0.046	aTPMS	15	57.0	6.3	58.6	5.9
0.058-0.061	aTPMS	12	61.0	4.6	63.1	5.8
0.079-0.10	aTPMS	14	65.3	4.8	66.8	5.0
0.11-0.12	aTPMS	10	69.6	6.8	74.6	7.3
0.14-0.14	aTPMS	16	73.9	5.7	76.2	4.9
0.28	aTPMS	4	84.0	2.9	84.9	7.4
0.46	aTPMS	2	81.7	4.9	87.9	1.4

*number of experiments, mean per experiment was calculated based on 3 retrodialysates and 4 dialysates

Abbreviations: aTPMS: artificial tissue perfusion microdialysis system; aTSMS: artificial tissue structure microdialysis system; SD: standard deviation.

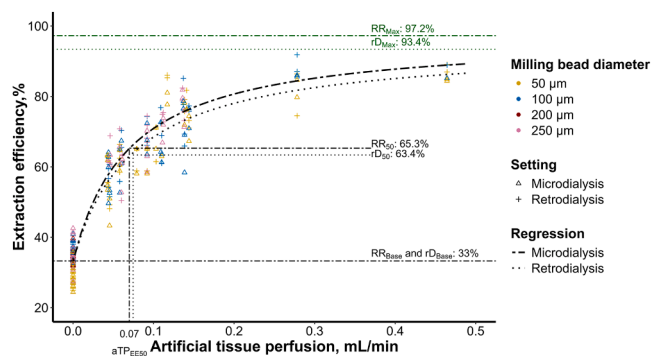


Fig. 6. Relationship between extraction efficiency (EE) and artificial tissue perfusion based on the artificial tissue perfusion microdialysis system and artificial tissue structure microdialysis system with estimated parameters for baseline (RR_{Base} and rD_{Base}), maximal extraction efficiency (RR_{Max} and rD_{Max}) as well as artificial tissue perfusion (aTP_{EE50}) corresponding to the half-maximal extraction efficiencies (RR₅₀ and rD₅₀) from nonlinear regression models. Lines display the regression for microdialysis setting (dashed) and retrodialysis (dotted), colours the milling bead sizes and symbols the setting.

3.5. Comparison of *in vitro* to *in vivo* reported extraction efficiencies

While aTSMS with an EE of 33.3 % underestimated the reported *in vivo* values for obese patients of 42.8 % and non-obese patients of 61.0 % (Bureau et al., 2019), the aTPMS reproduced the 95 % CI of the *in vivo* reported EE from 35.9 % to 50.2 % for obese and 54.4 % to 67.1 % for non-obese (Busse et al., 2021a): *In vitro* EE matched the *in vivo* EE of 42.8 % for obese patients at an aTP of 0.013 mL/min (95 %CI:0.0033–0.028 mL/min). The EE of 61.0 % for non-obese patients corresponded to a flow 0.061 mL/min (95 %CI:0.038–0.091 mL/min) (Eq. (4)). The same experimental µD setting (perfusate flow and catheter) was applied by Wiskirchen et al. in patients with diabetic foot infections investigating thigh and wound concentrations of LIN by µD. EE were 39.9 ± 14.6 % for thigh and 46.4 ± 17.3 % for wound catheters, corresponding to an aTP of 0.0088 and 0.020 mL/min, respectively.

4. Discussion

In this study a new *in vitro* µD system was developed to reproduce EE observed *in vivo*. The novel aTPMS was developed by introducing the catheter into a perfused MB matrix, which mimicked cellular tissue structure, and tissue perfusion. The aTPMS was developed in two steps: First the cellular structure was mimicked using MB, described as the aTSMS followed by the addition of the aTP through the MB matrix mimicking tissue perfusion, resulting in the aTPMS. The EE of LIN ranged from 33 % in the aTSMS to 91.5 % in the reference system, in which the matrix was a well-stirred solution. The EE of the aTPMS was within the range of the aTSMS and reference system and the impact of the aTP on the EE was best described by a saturable relationship.

4.1. Impact of milling beads on extraction efficiency

The inert spheres of the MB with controlled diameters formed a porous matrix with a free volume of 36.5 % (calculations based on the manufacturer's specified density and measured total volume). Free volume fraction between the MB is dependent on the packing and not the diameter and agreed well with an expected free volume of 36.5 % for typical bulk packing of spheres (Wu et al., 2003). Furthermore, the available volume for diffusion in the MB matrix was close to the ISF volume available for diffusion *in vivo*, which was estimated to be between 20 % and 40 % depending on the tissue and trauma caused by the insertion of µD catheters (Bungay et al., 2003; Dykstra et al., 1992). Considering the similar free volume around and between the MB and reported *in vivo* values as well as the high reproducibility of *in vivo*

observed EE in the aTPMS, MB were suitable to mimic the cellular structure and tortuosity.

In cases when RR and rD differed by >10 % ($n = 12$; 8 % of total 146 experiments) the data was excluded. Reasons for this may be: The position of the catheter in the MB matrix, if the catheter has been moved within the experiment, e.g. during the matrix sampling, EE may be affected. The MB did not allow a determination of the catheters position throughout the experiment. Another reason may have been remaining trapped air in the MB matrix close at the catheter membrane (Bureau et al., 2019). In 7 experiments μ D catheters malfunctioned. The most sensitive part was the connection of the catheter tubing with the semi-permeable membrane, which broke when compression along the vertical axis of the catheter was applied during catheter insertion into the surrounding matrix.

EE in the aTSMS decreased significantly from 91.5 % compared to the reference system of 33 %. In literature, a change in the rate limiting process from the permeability of the catheter surrounding matrix to the membrane permeability was described to cause the decrease in EE and can be assumed for the aTSMS (Bungay et al., 2006; Chen et al., 2002). In the aTSMS, LIN molecules distributed by diffusion in the catheter surrounding matrix which was hindered by MB, as LIN could only diffuse in the available space between the MB. As a consequence, LIN concentration may have depleted (RR) or accumulated (rD) in the vicinity of the membrane, resulting in the shown decrease of EE over time (Fig. 4 and Figure S2). The unexpected difference in EE between 50 μ m and larger MB may be attributed to changes in packing, which reduced free volume for diffusion or trapped air due to a more challenging filling process. In the aTSMS, larger MB diameters facilitated easier air removal in contrast to the 50 μ m MBs. The hydrophobic behaviour in combination with the surface tension of water caused 50 μ m MB to trap more air, resulting in air removal taking twice as long (30 min) compared to larger MBs to remove.

4.2. Extraction efficiencies in the aTPMS

The aTPMS allowed for an improved and time saving filling procedure. Benefit of the optimised filling was that the MB matrix was already in the desired test tube and did not need to be moved into another test tube as in the aTSMS setting, reducing the risk of reintroducing air. Thus, in the aTPMS, no significant difference between 50 μ m MB and larger MB was observed. For future applications, the use of larger MB diameters (>50 μ m) is recommended due to improved handling.

In contrast to the aTSMS, constant EE was achieved within experiments. The results indicated that the aTP prevented the accumulation or depletion of LIN around the catheter, supporting the assumption of a quasi-steady state, i.e. a constant concentration gradient between the vicinity of the catheter and nominal matrix concentration in the MB matrix, within the system after the 30 min equilibration time. At high aTP, this concentration gradient was assumed to be steeper compared to lower aTP (Bungay et al., 1989).

The characterised saturable relationship between aTP and EE revealed that all estimated parameters from the nonlinear regression model were comparable: Estimates of EE_{Max} (i.e. RR_{Max} and rD_{Max}) compared to the determined EE were slightly higher in the reference systems but agreeing well considering the variability. At lower aTP, the rate-limiting process was the matrix permeability of LIN. As aTP increased, the rate-limiting process shifted towards the membrane permeability. Consequently, with EE approaching the reference values, LIN C_{ISF} remained constant at the initial concentration (Figure S3). In the aTPMS, no solubility issues were expected due to the high aqueous solubility of LIN (3 mg/mL). However, *in vivo* LIN will diffuse from the retroperfusate (RS) into the ISF which may have a lower solubility compared to water, thus, it is advised to consider a suitable retroperfusate concentration of poorly soluble compounds to prevent altered EE due to solubility issues.

4.3. Comparison to *in vivo* reported extraction efficiencies

The aTP required to reproduce EE in ISF subcutaneous abdominal tissue for obese patients (EE:42.8 %) was lower with 0.0013 mL/min compared to non-obese patients (EE:61.0 %) with aTP of 0.061 mL/min. From a physiological perspective in abdominal subcutaneous adipose tissue blood flow in obese patients was reported at 1.75 mL/min/100 g tissue and differed significantly by a factor of ~2.5 to non-obese patients with 4.38 mL/min/100 g tissue (Summers et al., 1996). These results agreed well with the ~4.7-fold difference in aTP in the aTPMS for obese and non-obese, indicating that a lower tissue perfusion was most likely the reason for the reduced EE in obese patients. Furthermore, Summer et al. reported a high variability in blood flow not only between patients but also within patients if determined at different occasions (Summers et al., 1996): Blood flow in subcutaneous abdominal tissue for non-obese varied from 0.98 to 7.69 mL/min/100 g tissue and obese from 0.60 to 3.55 mL/min/100 g tissue, providing a potential explanation for high retrodialysis-related variability observed in clinical μ D studies (Busse et al., 2021a). The increased EE in infected tissue compared to healthy tissue in the study from Wiskirchen et al. may be explained by an increased tissue perfusion or increase in ISF volume due to the inflammation (Wiskirchen et al., 2011). Furthermore, Buerger et al. estimated LIN EE (perfusate flow 1.5 μ L/min) in subcutaneous adipose tissue and muscles with 53.1 % (CV=31 %) and 59.1 % (CV=17 %), respectively (Buerger et al., 2006). Even though no significant difference between the two tissues was found, the higher EE and lower CV in muscles may be a result of the higher and less variable tissue perfusion of the muscle tissue compared to adipose tissue.

4.4. Application criteria for the aTPMS

The aTPMS effectively mimicked a scenario for substances where tissue permeability, thus EE, was driven by diffusion in the tissue ISF and elimination from the tissue into the vascular system. The aTPMS is applicable for exogenous substances like LIN, which will not intensively be metabolised in the tissue (ISF and intracellular), distribution into cells is fast and in equilibrium (Bungay et al., 1989; Pascual et al., 2002), and no additional diffusion barrier like the blood brain barrier is present, EE depends on tissue permeability, thus blood flow and D_t (Morgan and Huang, 1993). However, additional processes as metabolism and active transport will increase tissue permeability (Bungay et al., 2006) and are not represented in the aTPMS. Consequently, the determined EE by the aTPMS may be lower than the expected *in vivo* EE, when e.g. metabolism contributes significantly to the tissue permeability *in vivo*. Furthermore, differences between the D_t in the extracellular matrix *in vivo* and the RS used *in vitro* in the aTPMS are to be expected. This is relevant for large molecules, as they interact with molecules within the extracellular matrix decreasing D_t , whereas for small molecules less interaction between the substance and extracellular matrix is expected. Thus, for small molecules D_t is mainly depending on tortuosity and the available free volume (Syková and Nicholson, 2008). Additionally, around the catheter a layer of unstirred water is present which may have an impact on the permeability of LIN in the catheter surrounding matrix (Korjamo et al., 2009). The thickness of the unstirred water layer is decreased by smaller MB sizes and higher aTP. As there was no relevant difference in EE between MB diameters in the aTPMS, the impact of the unstirred water layer thickness on tissue permeability was assumed to be smaller compared to the elimination by aTP. However, these additional mechanism as well as the fact that the applied aTP was lower compared to the reported blood flows *in vivo*, a direct translation to blood flow will require further investigations. If the aTPMS can be used for other substances that fulfil application criteria needs to be evaluated.

4.5. Future perspectives

Understanding the impact of D_t and tissue perfusion on the EE is

essential when planning clinical μ D studies and analysing μ D-related data. When determining EE in retrodialysis, the assumption is made that EE does not change during μ D sampling. If fundamental changes in tissue perfusion are expected to occur during the study, *i.e.* to anaesthesia and surgery, or in not yet studied populations, the range of expected EE should be investigated to support μ D setting design in future investigation. Especially tissue distribution in vulnerable populations is important and often only few individuals are included in μ D studies, highlighting the importance of the μ D setting and the underlying assumptions. The application of the aTPMS to new substances is promising, as substances with similar tissue permeability have been shown to exhibit similar EE *in vivo* and are already used for “calibration by internal standard”, an extension of the retrodialysis method (Bouw and Hammarlund-Udenaes, 1998; Knudsen et al., 2021; Lee et al., 2003). Thus, the principle is likely transferable to the aTPMS as well.

5. Conclusion

A novel *in vitro* μ D system was developed to reproduce *in vivo* EE by incorporating a MB matrix that mimicked cellular diffusion barriers, and a flow mimicking tissue perfusion. The system demonstrated that EE increased with increasing aTP, reflecting real-world scenarios where tissue perfusion may vary. The results indicated that in poorly perfused tissues or when tissue perfusion changes, EE may fluctuate, challenging the assumption that retrodialysis EE remains constant during sampling. To account for a changing EE, it would be essential to monitor rate-limiting processes like tissue perfusion in clinical μ D studies, in this respect the ethanol technique presents a promising option (Wallgren et al., 1995). The novel aTPMS offers a promising approach to systematically investigate differences in EE observed *in vivo* caused by varying tissue perfusions, particularly for LIN, and can support the design of clinical trials, *e.g.* in new study populations or when different μ D catheters need to be used. A broader application of the novel aTPMS is proposed as well as the comparison to *in vivo* μ D data to other substances, with tissue distribution mainly driven by diffusion and not undergoing metabolism.

Declaration of generative AI and AI-assisted technologies in the writing process

During the preparation of this work the author(s) used GPT-4o (openAI, San Francisco, US) in order to improve understandability and proof reading. After using this tool, the author(s) reviewed and edited the content as needed and take(s) full responsibility for the content of the publication

CRediT authorship contribution statement

Felix Leon Müller: Writing – review & editing, Writing – original draft, Visualization, Methodology, Investigation, Formal analysis. **Davide Bindellini:** Writing – review & editing, Methodology. **Gerd Mikus:** Writing – review & editing, Visualization, Supervision. **Robin Michelet:** Writing – review & editing, Visualization, Supervision, Formal analysis. **Charlotte Kloft:** Writing – review & editing, Visualization, Supervision, Methodology, Conceptualization.

Declaration of competing interest

Charlotte Kloft received research grants from an industry consortium (AbbVie Deutschland GmbH & Co. K.G., AstraZeneca, Boehringer Ingelheim Pharma GmbH & Co. KG., Gruenthal GmbH, F. Hoffmann-La Roche Ltd., Merck KGaA, Novo Nordisk A/S and Sanofi) for the graduate research training program PharMetrX, from the Innovative Medicines Initiative-Joint Undertaking (“DDMoRe”), from H2020-EU.3.1.3 (“FAIR”), Diurnal Ltd. and the Federal Ministry of Education and Research within the Joint Programming Initiative on Antimicrobial

Resistance Initiative (“JPIAMR”), all outside the submitted work. All other authors declare no competing interest for this work.

Funding sources

Open Access funding enabled and organized by Projekt DEAL.

Acknowledgments

The author expresses gratitude to Tania Fuhrmann Selter for her support in conducting the experiments. Additionally, appreciation is extended to the Freie Universität Berlin for the financial support, as well as to all involved for the many productive discussions.

Supplementary materials

Supplementary material associated with this article can be found, in the online version, at doi:10.1016/j.ejps.2025.107085.

Data availability

Data will be made available on request.

References

- Andreas, M., Zeitlinger, M., Wissner, W., Jaeger, W., Maier-Salamon, A., Thalhammer, F., Kocher, A., Hiesmayr, J.M., Laufer, G., Hutschala, D., 2015. Cefazolin and linezolid penetration into sternal cancellous bone during coronary artery bypass grafting. *Euro. J. Cardio-Thoracic Surg.* 48, 758–764. <https://doi.org/10.1093/ejcts/ezu491>.
- Bouw, M.R., Hammarlund-Udenaes, M., 1998. Methodological aspects of the use of a calibrator in *In vivo* microdialysis—Further development of the retrodialysis method. *Pharm. Res.* 15, 1673–1679. <https://doi.org/10.1016/j.jchromb.2003.08.019>.
- Buerger, C., Joukhadar, C., Muller, M., Kloft, C., 2003. Development of a liquid chromatography method for the determination of linezolid and its application to *in vitro* and human microdialysis samples. *J. Chromatogr. B Analyt. Technol. Biomed. Life Sci.* 796, 155–164. <https://doi.org/10.1016/j.jchromb.2003.08.019>.
- Buerger, C., Plock, N., Dehghanyar, P., Joukhadar, C., Kloft, C., 2006. Pharmacokinetics of unbound linezolid in plasma and tissue interstitium of critically ill patients after multiple dosing using microdialysis. *Antimicrob. Agents Chemother.* 50, 2455–2463. <https://doi.org/10.1128/AAC.01468-05>.
- Bungay, P.M., Dedrick, R.L., Fox, E., Balis, F.M., 2001. Probe calibration in transient microdialysis *In vivo*. *Pharm. Res.* 361–366. <https://doi.org/10.1023/A:1011015316327>.
- Bungay, P.M., Morrison, P.F., Dedrick, R.L., 1989. Steady-state theory for quantitative microdialysis of solutes and water *in vivo* and *in vitro*. *Life Sci.* 46, 105–119. [https://doi.org/10.1016/0024-3205\(90\)90043-q](https://doi.org/10.1016/0024-3205(90)90043-q).
- Bungay, P.M., Morrison, P.F., Dedrick, R.L., Chefer, V.I., Zapata, A., 2006. Chapter 2.2 principles of quantitative microdialysis. *Handbook of Behavioral Neuroscience*, pp. 131–167. [https://doi.org/10.1016/S1569-7339\(06\)16008-7](https://doi.org/10.1016/S1569-7339(06)16008-7).
- Bungay, P.M., Newton-Vinson, P., Isele, W., Garris, P.A., Justice Jr, J.B., 2003. Microdialysis of dopamine interpreted with quantitative model incorporating probe implantation trauma. *J. Neurochem.* 86, 932–946. <https://doi.org/10.1046/j.1471-4159.2003.01904.x>.
- Burau, D., Petroff, D., Simon, P., Ehmann, L., Weiser, C., Dorn, C., Kratzer, A., Wrigge, H., Kloft, C., 2019. Drug combinations and impact of experimental conditions on relative recovery in *in vitro* microdialysis investigations. *Euro. J. Pharmaceut. Sci.* 127, 252–260. <https://doi.org/10.1016/j.ejps.2018.10.030>.
- Busse, D., Simon, P., Michelet, R., Ehmann, L., Mehner, F., Dorn, C., Kratzer, A., Huisinga, W., Wrigge, H., Petroff, D., Kloft, C., 2021a. Quantification of microdialysis related variability in humans: clinical trial design recommendations. *Euro. J. Pharmaceut. Sci.* 157, 105607. <https://doi.org/10.1016/j.ejps.2020.105607>.
- Busse, D., Simon, P., Petroff, D., Dorn, C., Schmitt, L., Bindellini, D., Kratzer, A., Dietrich, A., Zeitlinger, M., Huisinga, W., Michelet, R., Wrigge, H., Kloft, C., 2021b. Similar piperacillin/tazobactam target attainment in obese versus non-obese patients despite differences in interstitial tissue fluid pharmacokinetics. *Pharmaceutics*. 13, 1380. <https://doi.org/10.3390/pharmaceutics13091380>.
- Busse, D., Simon, P., Schmitt, L., Petroff, D., Dorn, C., Dietrich, A., Zeitlinger, M., Huisinga, W., Michelet, R., Wrigge, H., Kloft, C., 2021. Comparative plasma and interstitial tissue fluid pharmacokinetics of Meropenem demonstrate the need for increasing dose and infusion duration in obese and non-obese patients. *Clin. Pharmacokinet.* 61, 655–672. <https://doi.org/10.1007/s40262-021-01070-6>.
- Chen, K.C., Höistad, M., Kehr, J., Fuxe, K., Nicholson, C., 2002. Theory relating *in vitro* and *in vivo* microdialysis with one or two probes. *J. Neurochem.* 81, 108–121. <https://doi.org/10.1046/j.1471-4159.2002.00793.x>.
- Craig, W.A., Middleton, W.S., 1998. Pharmacokinetic/pharmacodynamic parameters: rationale for antibacterial dosing of mice and men. *Clinic. Infect. Dis.* 26, 1–12. <https://doi.org/10.1086/516284>.

- De La Pena, A., Liu, P., Derendorf, H., 2000. Microdialysis in peripheral tissues. *Adv. Drug Deliv. Rev.* 45, 189–216. [https://doi.org/10.1016/S0169-409X\(00\)00106-X](https://doi.org/10.1016/S0169-409X(00)00106-X).
- Dehghanyar, P., Bürger, C., Zeitlinger, M., Islinger, F., Kovar, F., Müller, M., Kloft, C., Joukhadar, C., 2005. Penetration of linezolid into soft tissues of healthy volunteers after single and multiple doses. *Antimicrob. Agents Chemother.* 49, 2367–2371. <https://doi.org/10.1128/AAC.49.6.2367-2371.2005>.
- Deitchman, A.N., Singh, R.S.P., Derendorf, H., 2018. Nonlinear protein binding: not what you think. *J. Pharm. Sci.* 107, 1754–1760. <https://doi.org/10.1016/j.xphs.2018.03.023>.
- Dykstra, K.H., Hsiao, J.K., Morrison, P.F., Bungay, P.M., Mefford, I.N., Scully, M.M., Dedrick, R.L., 1992. Quantitative examination of tissue concentration profiles associated with microdialysis. *J. Neurochem.* 58, 931–940. <https://doi.org/10.1111/j.1471-4159.1992.tb09346.x>.
- Ehmann, L., Simon, P., Busse, D., Petroff, D., Dorn, C., Huisinga, W., Dietrich, A., Zeitlinger, M., Wrigge, H., Kloft, C., 2020. Risk of target non-attainment in obese compared to non-obese patients in calculated linezolid therapy. *Clinic. Microbiol. Infect.* 26, 1222–1228. <https://doi.org/10.1016/j.cmi.2020.04.009>.
- Eslam, R.B., Burian, A., Vila, G., Sauerermann, R., Hammer, A., Frenzel, D., Minichmayr, I. K., Kloft, C., Matzneller, P., Oesterreicher, Z., Zeitlinger, M., 2014. Target site pharmacokinetics of linezolid after single and multiple doses in diabetic patients with soft tissue infection. *J. Clin. Pharmacol.* 54, 1058–1062. <https://doi.org/10.1002/jcph.296>.
- Gee, T., Ellis, R., Marshall, G., Andrews, J., Ashby, J., Wise, R., 2001. Pharmacokinetics and tissue penetration of linezolid following multiple oral doses. *Antimicrob. Agents Chemother.* 45, 1843–1846. <https://doi.org/10.1128/AAC.45.6.1843-1846.2001>.
- Kho, C.M., Rahim, S.K.E.A., Ahmad, Z.A., Abdullah, N.S., 2017. A review on microdialysis calibration methods: the theory and current related efforts. *Mol. Neurobiol.* <https://doi.org/10.1007/s12035-016-9929-8>.
- Knudsen, M.B., Bue, M., Pontoppidan, L.L., Hvistendahl, M.A., Søballe, K., Stilling, M., Hanberg, P., 2021. Evaluation of benzylpenicillin as an internal standard for measurement of piperacillin bone concentrations via microdialysis. *J. Pharm. Sci.* 110, 3500–3549. <https://doi.org/10.1016/j.xphs.2021.06.008>.
- Korjamo, T., Heikkinen, A.T., Mönkkönen, J., 2009. Analysis of unstirred water layer in *in vitro* permeability experiments. *J. Pharm. Sci.* 98, 4469–4479. <https://doi.org/10.1002/jps.21762>.
- Lee, K.J., Mower, R., Hollenbeck, T., Castelo, J., Johnson, N., Gordon, P., Sinko, P.J., Holme, K., Lee, Y.H., 2003. Modulation of nonspecific binding in ultrafiltration protein binding studies. *Pharm. Res.* 20, 1015–1021. <https://doi.org/10.1023/A:1024406221962>.
- Marchand, S., Chauzy, A., Dahyot-Fizelier, C., Couet, W., 2016. Microdialysis as a way to measure antibiotics concentration in tissues. *Pharmacol. Res.* 111, 201–207. <https://doi.org/10.1016/j.phrs.2016.06.001>.
- Morgan, D.J., Huang, J.L., 1993. Effect of plasma protein binding on kinetics of capillary uptake and efflux. *Pharm. Res.* 10, 300–304. <https://doi.org/10.1023/A:1018959415963>.
- Nation, R.L., Theuretzbacher, U., Tsuji, B.T., 2018. Concentration-dependent plasma protein binding: expect the unexpected. *Euro. J. Pharmaceut. Sci.* 122, 341–346. <https://doi.org/10.1016/j.ejps.2018.07.004>.
- Nilsson, L.B., 2013. The bioanalytical challenge of determining unbound concentration and protein binding for drugs. *Bioanalysis.* 5, 3033–3050. <https://doi.org/10.4155/bio.13.274>.
- Pascual, Á., Ballesta, S., García, I., Perea, E.J., 2002. Uptake and intracellular activity of linezolid in human phagocytes and nonphagocytic cells. *Antimicrob. Agents Chemother.* 46, 4013–4015. <https://doi.org/10.1128/AAC.46.12.4013-4015.2002>.
- Plock, N., Kloft, C., 2005. Microdialysis - theoretical background and recent implementation in applied life-sciences. *Euro. J. Pharmaceut. Sci.* 25, 1–24. <https://doi.org/10.1016/j.ejps.2005.01.017>.
- Ryan, D.M., 1993. Pharmacokinetics of antibiotics in natural and experimental superficial compartments in animals and humans. *J. Antimicrob. Chemother.* 31, 1–16. <https://doi.org/10.1093/jac/31.suppl.d.1>.
- Schwameis, R., Syré, S., Sarahrudi, K., Appelt, A., Marhofer, D., Burau, D., Kloft, C., Zeitlinger, M., 2017. Penetration of linezolid into synovial fluid and muscle tissue after elective arthroscopy. *J. Antimicrob. Chemother.* 72, 2817–2822. <https://doi.org/10.1093/jac/dkx219>.
- Simmel, F., Kirbs, C., Erdogan, Z., Lackner, E., Zeitlinger, M., Kloft, C., 2013. Pilot investigation on long-term subcutaneous microdialysis: proof of principle in humans. *AAPS J* 15 (1), 95–103. <https://doi.org/10.1208/s12248-012-9412-z>.
- Stenzen, J.A., 1999. Methods and issues in microdialysis calibration. *Anal. Chim. Acta* 179, 337–358. [https://doi.org/10.1016/S0003-2670\(98\)00598-4](https://doi.org/10.1016/S0003-2670(98)00598-4).
- Stolle, L.B., Plock, N., Joukhadar, C., Arpi, M., Emmertsen, K.J., Buerger, C., Riegels-Nielsen, P., Kloft, C., 2008. Pharmacokinetics of linezolid in bone tissue investigated by *in vivo* microdialysis. *Scand. J. Infect. Dis.* 40, 24–29. <https://doi.org/10.1080/00365540701509873>.
- Summers, L.K.M., Samra, J.S., Humphreys, S.M., Morris, R.J., Frayn, K.N., 1996. Subcutaneous abdominal adipose tissue blood flow: variation within and between subjects and relationship to obesity. *Clin. Sci.* 9, 679–683. <https://doi.org/10.1042/cs0910679>.
- Syková, E., Nicholson, C., 2008. Diffusion in brain extracellular space. *Physiol. Rev.* 88, 1277–1340. <https://doi.org/10.1152/physrev.00027.2007>.
- Thallinger, C., Buerger, C., Plock, N., Kljucar, S., Wuenscher, S., Sauerermann, R., Kloft, C., Joukhadar, C., 2008. Effect of severity of sepsis on tissue concentrations of linezolid. *J. Antimicrob. Chemother.* 61, 173–176. <https://doi.org/10.1093/jac/dkm431>.
- van Os, W., Nussbaumer-Pröll, A., Pham, A.D., Wijnant, G.J., Ngougni Pokem, P., Van Bambeke, F., van Hasselt, J.G.C., Zeitlinger, M., 2024. Pharmacokinetic/pharmacodynamic model-based optimization of temocillin dosing strategies for the treatment of systemic infections. *J. Antimicrobial Chemother.* dkae243. <https://doi.org/10.1093/jac/dkae243>.
- van Os, W., Zeitlinger, M., 2021. Predicting antimicrobial activity at the target site: pharmacokinetic/pharmacodynamic indices *versus* time–Kill approaches. *Antibiotics* 10, 1485. <https://doi.org/10.3390/antibiotics10121485>.
- Wallgren, F., Amberg, G., Hickner, R.C., Ekelund, Ulf, Jorfeldt, L., Henriksson, J., Hickner, R.C., Ekelund, Ulf, Henriks, J., 1995. A mathematical model for measuring blood flow in skeletal muscle with the microdialysis ethanol technique. *J. Appl. Physiol.* 648–659. <https://doi.org/10.1152/jappl.1995.79.2.648>.
- Wiskirchen, D.E., Shepard, A., Kuti, J.L., Nicolau, D.P., 2011. Determination of tissue penetration and pharmacokinetics of linezolid in patients with diabetic foot infections using *in vivo* microdialysis. *Antimicrob. Agents Chemother.* 55, 4170–4175. <https://doi.org/10.1128/AAC.00445-11>.
- Wu, Y., Fan, Z., Lu, Y., 2003. Bulk and interior packing densities of random close packing of hard spheres. *J. Mater. Sci.* 38, 2019–2025. <https://doi.org/10.1023/A:1023597707363>.
- Zhao, Y., Liang, X., Lunte, C.E., 1995. Comparison of recovery and delivery *in vitro* for calibration of microdialysis probes. *Anal. Chim. Acta* 316, 403–410. [https://doi.org/10.1016/0003-2670\(95\)00379-E](https://doi.org/10.1016/0003-2670(95)00379-E).